Recognition and Resistance in TEM β-Lactamase[†]

Xiaojun Wang,[‡,§,||] George Minasov,[‡,§,⊥] Jesús Blázquez,[#] Emilia Caselli,[&] Fabio Prati,[&] and Brian K. Shoichet*[,§]

Department of Pharmaceutical Chemistry, University of California San Francisco, Genentech Hall, San Francisco, California 94143, Servicio de Microbiologia, Hospital Ramón y Cajal, Madrid, Spain, and Dipartimento di Chimica, Universitá degli studi di Modena, via Campi 183, Modena, Italy

Received February 12, 2003; Revised Manuscript Received May 27, 2003

ABSTRACT: Developing antimicrobials that are less likely to engender resistance has become an important design criterion as more and more drugs fall victim to resistance mutations. One hypothesis is that the more closely an inhibitor resembles a substrate, the more difficult it will be to develop resistant mutations that can at once disfavor the inhibitor and still recognize the substrate. To investigate this hypothesis, 10 transition-state analogues, of greater or lesser similarity to substrates, were tested for inhibition of TEM-1 β-lactamase, the most widespread resistance enzyme to penicillin antibiotics. The inhibitors were also tested against four characteristic mutant enzymes: TEM-30, TEM-32, TEM-52, and TEM-64. The inhibitor most similar to the substrate, compound **10**, was the most potent inhibitor of the WT enzyme, with a K_i value of 64 nM. Conversely, compound **10** was the most susceptible to the TEM-30 (R244S) mutant, for which inhibition dropped by over 100-fold. The other inhibitors were relatively impervious to the TEM-30 mutant enzyme. To understand recognition and resistance to these transition-state analogues, the structures of four of these inhibitors in complex with TEM-1 were determined by X-ray crystallography. These structures suggest a structural basis for distinguishing inhibitors that mimic the acylation transition state and those that mimic the deacylation transition state; they also suggest how TEM-30 reduces the affinity of compound **10**. In cell culture, this inhibitor reversed the resistance of bacteria to ampicillin, reducing minimum inhibitory concentrations of this penicillin by between 4- and 64-fold, depending on the strain of bacteria. Notwithstanding this activity, the resistance of TEM-30, which is already extant in the clinic, suggests that there can be resistance liabilities with substrate-based design.

Confronted by an enzyme prone to resistance mutations, is it better to design inhibitors that resemble the substrate or to design inhibitors dissimilar to the substrate? This is a pressing question in antiviral and antibacterial chemotherapy, where there is often considerable pressure for targets to mutate (*1*, *2*). Colman and colleagues have argued persuasively that substrate-analogue inhibitors will be difficult to distinguish from the substrate, and since the enzyme must still recognize the substrate, this should make a successful resistance substitution difficult (*3*). This "substrate-analog" hypothesis thus suggests that the more similar an inhibitor is to a substrate, the more difficult it will be to find a mutant enzyme that confers resistance to that inhibitor while maintaining enough activity against the substrate to be viable. We might also consider a "novel inhibitor" hypothesis that turns the substrate-analog argument on its head: the enzyme is already good at substrate recognition, and so it will take only subtle changes to convert a substrate analogue into a substrate, or to modify specific recognition residues to attenuate inhibition. This might be most problematic when substrate analogue inhibitors have already been widely used and mutant enzymes have had a chance to evolve against them. Such pre-evolved resistance would not pose a threat to novel inhibitors.

For resistance to β-lactam antibiotics, such as penicillins and cephalosporins, unintentional experiments that speak to this question have been taking place in the clinic since the 1940s. Soon after penicillin was introduced, bacteria resistant to it were observed (*4*) and were eventually shown to produce a class A β-lactamase enzyme that hydrolyzed the eponymous β-lactam ring, inactivating the drugs. β-Lactamases, such as the plasmid-borne TEM-1, spread with the use of penicillins, cephalosporins, and related β-lactams (*5*). To combat these enzymes, mechanism-based inhibitors, such as clavulanate (Figure 1), were introduced (*6*), followed by "β-lactamase-stable" compounds such as third-generation cephalosporins (*7*). Both classes are themselves β-lactams and resemble the original substrates.

In response to these inhibitors and "β-lactamase resistant" compounds, mutant TEM β-lactamases began to appear in the clinic; over 100 of these have been characterized since 1983 (www.lahey.org/studies/temtable.htm). Inhibitor-resistant TEM (IRT) mutants such as TEM-30, TEM-32, and TEM-34 confer resistance to clinically used β-lactamase

[†] This work was supported by G.M.63815 from the NIH (to B.K.S.).
* Corresponding author. E-mail: shoichet@cgl.ucsf.edu. Phone: 312-503-0081. Fax: 312-503-5349.
[‡] These authors contributed equally to this paper.
[§] University of California San Francisco.
[||] Current address: Abbott Laboratories, AP10-1, R4CK, GPRD, 100 Abbott Park Road, Abbott Park, IL 60064-3502.
[⊥] Current address: Department of MPBC, Northwestern University, 303 E. Chicago Ave., Chicago, IL 60611.
[#] Servicio de Microbiologia.
[&] Universitá degli studi di Modena.

[1] Abbreviations: WT*, TEM-1 mutant M182T; MIC, minimum inhibitory concentration; AMP, ampicillin; IRT, inhibitor-resistant TEM; ESBL, extended spectrum β-lactamase.

10.1021/bi034242y CCC: $25.00
Published on Web 06/24/2003

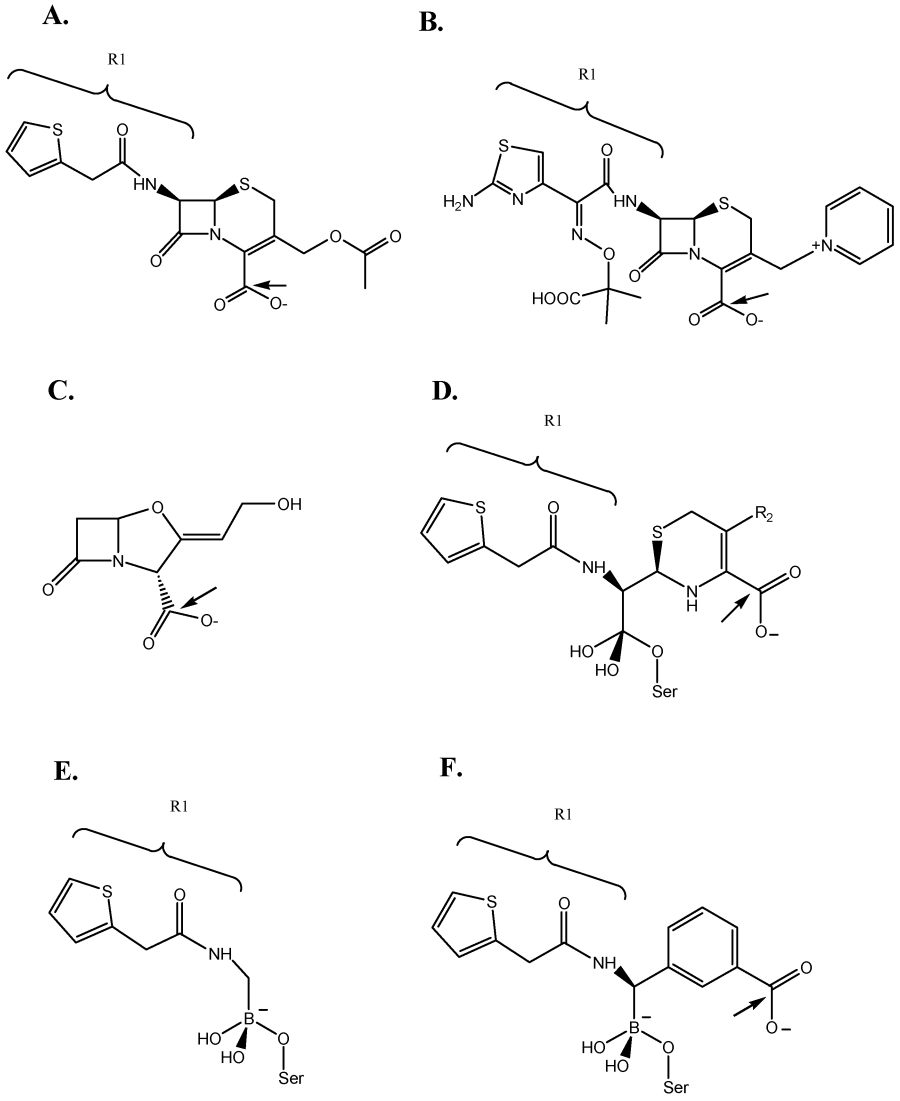

FIGURE 1: β-Lactams and β-lactamase inhibitors. The C4′ carboxylates and analogous *m*-carboxylates are identified by an arrow. A. The substrate cephalothin. B. The "β-lactamase-stable" cephalosporin ceftazidime. C. The inhibitor clavulanate. D. Deacylation high-energy intermediate for cephalothin. E. The acylation transition-state analogue **10a**. F. The deacylation transition-state analogue **10**.

inhibitors such as clavulanate. Extended spectrum β-lactamase (ESBL) mutants such as TEM-10, TEM-52, and TEM-64 confer resistance to third-generation cephalosporins. Both classes of mutant enzymes have arisen through only a few substitutions and either avoid or simply hydrolyze the inhibitors and "β-lactamase-stable" drugs. Considerable literature now exists on the clinical manifestations, mechanisms of action, evolutionary relationships, and structures of these mutant enzymes (see reviews by Knowles (*8*), Yang (*9*), Matagne (*10*), and Knox (*11*)). In addition, most inhibitors and "β-lactamase-stable" drugs are either relatively inactive against or susceptible to Class C β-lactamases, such as AmpC, which, like the TEM mutants, are increasingly prevalent in the clinic (*12*).

Although inhibitors and "β-lactamase-stable" compounds are substrate-analogues, they are imperfect compounds to test stability to resistance mutants. β-Lactamases have only had to lose off-pathway—and, hence for substrates, unimportant—reactions to become resistant to mechanism-based inhibitors such as clavulanate. Similarly, "β-lactamase-stable" compounds such as cefotaxime are thought to be too large to bind in the β-lactamase site in a catalytically competent configuration—resistance has arisen through substitutions that simply enlarge the active site, allowing the enzymes to hydrolyze these compounds as they would any other β-lactam. Inhibitors that are hydrolytically inert would overcome this problem, since the enzymes would not be able to mutate to convert them into substrates and would provide a better test for the substrate-analog hypothesis. For serine β-lactamases, such as TEM, an example of such nonhydrolyzable inhibitors are boronic acid transition-state analogues (*13*−*18*). These molecules adopt a stable tetrahedral adduct when bound to the catalytic serine (Figure 1E,F), reversibly inhibiting β-lactamases. Both boronic acids and the related phosphonic acids (*19*, *20*) can inhibit serine β-lactamases tightly, reaching K_i values in the 1 to 10 nM range (*14*, *17*, *18*).

We have found that transition-state analogues that display more substrate groups have higher affinity for the class C β-lactamase AmpC. For instance, compound **10a** (Figure 1E) is a boronic acid that bears about half of the recognition elements found in most β-lactams, the R1 side chain of the cephalosporin cephalothin (Figure 1A), and is a 300 nM inhibitor of AmpC (*16*). Compound **10** (Figure 1F) is a

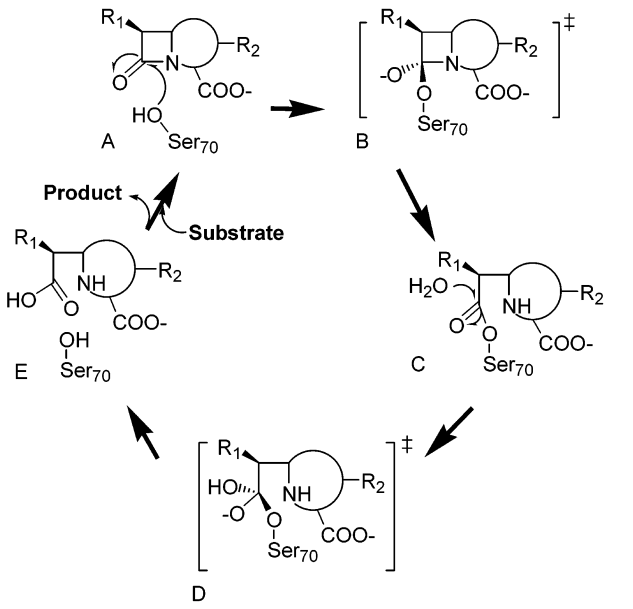

FIGURE 2: The reaction cycle of TEM-1 β-lactamase. A. The first-encounter, pre-covalent complex. B. The acylation high-energy intermediate. C. The acyl−enzyme complex. D. The deacylation high-energy intermediate. E. The product complex.

boronic acid that displays both the cephalothin side chain and a group from the other half of a β-lactam substrate, the C3(4)′ carboxylate, and is a 1 nM inhibitor of AmpC (*18*). Having designed **10** against AmpC, we wondered whether it would also be active against class A β-lactamases. The compound would need to inhibit both classes of enzymes to have wide clinical impact, and compound **10a**, its predecessor, was only a 7 μM inhibitor of TEM-1 (*16*). If compound **10** did inhibit the class A β-lactamases potently, we were interested to learn the structural bases of recognition. Transition state analogues can adopt two different orientations in the binding sites of class A β-lactamases, mimicking either the acylation transition state (Figure 2B) (*21*, *22*) or the deacylation transition state (Figure 2D) (*14*); we wanted to understand what inhibitor groups determined the transition state that was mimicked. Most importantly, we wondered how active compound **10** would be against the mutant IRT and ESBL TEM enzymes.

Here we investigate these questions by determining the affinity of compound **10** and nine analogues against TEM-1 and four characteristic mutant enzymes: two IRTs, TEM-30 and TEM-32, and two ESBLs, TEM-52 and TEM-64. To understand the bases of affinity, we determine X-ray crystal structures of four of these compounds, including compound **10**, in complex with TEM-1. We find that whereas compound **10** shows high affinity for TEM-1 and can reverse TEM-mediated resistance in bacterial cell culture, its affinity is dramatically attenuated by at least one of the known mutant enzymes. The implications for inhibitor design and the evolution of resistance will be considered.

MATERIALS AND METHODS

Preparation of TEM-1 Mutants. The enzymes used in this study included: TEM-1 wild type (WT); the stability mutant M182T, which we will refer to as WT* (see below) (*22*); TEM-30 (R244S); TEM-32 (M69I/M182T); TEM-52 (E104K/M182T/G238S); and TEM-64 (E104K/R164S/M182T). All were cloned, expressed, and purified as previously described (*22*, *23*).

Enzyme Kinetics. The enzyme assay was carried out in 50 mM potassium phosphate, pH 7.0 at room temperature. Concentrations were determined using the extinction coefficients of the mutant enzymes, diluted from stock solutions, and the substrates, as described (*23*). The values of k_{cat} and K_M were determined by initial velocity nonlinear regression analysis ($v_o = k_{cat}\cdot S/(K_M+S)$) using KaleidaGraph (Synergy Software, Reading, PA). The different mutants had different substrate specificities and activities and different enzyme concentrations and substrates were used for each. For TEM-1, 10 nM enzyme was used with 500 μM cephalothin (Sigma) (K_m = 180 μM) as the initial substrate concentration. For TEM-64, 11 nM enzyme and 300 μM cephalothin (K_m = 110 μM). For TEM-52, 4 nM of enzyme was used with 300 μM cefotaxime (Sigma) (K_m = 80 μM) as the initial substrate concentration. For TEM-30, 0.5 nM of enzyme was used with 300 μM nitrocefin (Oxoid) (K_m = 420 μM) as the initial substrate concentration. For TEM-32, 3 nM of enzyme was used with 300 μM nitrocefin (Km = 95 μM) as the initial substrate concentration. The hydrolysis of cephalothin and cefotaxime were monitored at 260 nm, and that of nitrocefin was monitored at 480 nm. All assays were initiated by the addition of enzyme, except for the *m*-carboxyphenylglycylboronic acids **8**, **9**, and **10**. For these three, a pronounced incubation effect was observed, and so the enzymes were allowed to preincubate with the inhibitors for five minutes before the reactions were initiated by addition of substrate. For these *m*-carboxyphenylglycylboronic acids, inhibition rates were measured after the reactions had reached a steady state rate (i.e., after the initial lag typical of slow off-rate reactions had been overcome), typically by using the final 20 s of a 300 s reaction. K_i values were determined using progress curves, which have been shown to be accurate for boronic acid inhibitors of β-lactamases (*13*, *15*, *16*, *18*). Typically, progress curves at 50% inhibition were compared to uninhibited curves using the method of Waley (*13*); for compounds **8**, **9**, and **10**, progress curves for reactions inhibited at the 80% level were used.

Crystallization and Data Collection. Crystals were grown using micro-seeding techniques. Most of the complexes were grown with mutant M182T as a proxy for TEM-1 WT. This enzyme is isofunctional with TEM-1, but is more stable and diffracts to a higher resolution (*24*, *25*), and for this reason was used in the crystallographic experiments. We will refer to this enzyme as WT*. An 8 μL droplet containing about 3−5 mg/mL of the enzyme and 2.5−3.0 mM boronic acid inhibitors in 0.65−0.70 M sodium−potassium phosphate buffer, pH 8.3, was seeded with micro crystals of apo-WT* (*23*) or TEM-64 (*25*) and placed over 1.4 M sodium−potassium phosphate well buffer, pH 8.3. Single crystals appeared in about two weeks and grew to a maximum size in two weeks. Crystals were soaked in cryoprotectant (25% sucrose in 1.6 M phosphate buffer, pH 8.3) for less than 60 s and then flash-cooled in liquid nitrogen. Diffraction data were collected from single crystals on the 5ID beamline of the DND-CAT at Advanced Photon Source (Argonne, IL). Single-wavelength data were measured at different energies using a MARCCD detector (Table 2). Reflections were integrated, scaled, and merged using the HKL package

Table 1: Inhibition of TEM-1 and Its Mutants by Transition-State Analogs

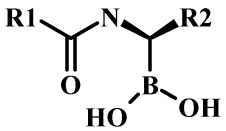

			K_i values against mutant TEMs (μM)[a]				
compound	R1	R2	TEM-1	TEM-30	TEM-32	TEM-52	TEM-64
1	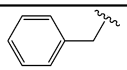	H	41	32	38	43	75
2	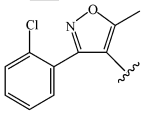	H	21	18	26	22	20
3	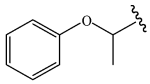	H	6.7	3.9	7.1	4.3	16
4	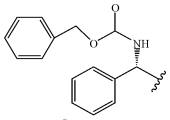	H	6.4	2.4	1.8	2.4	36
5	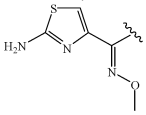	H	4.0	3.7	2.9	1.1	14
6	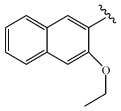	H	1.4	1.3	1.7	11	3.3
7	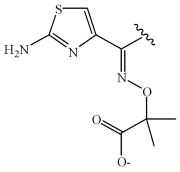	H	0.51	3.1	1.1	3.0	1.6
8	-CH_3	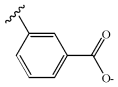	3.2	290	6.5	8.7	11
8a[b]	-CH_3	H	165	NT[c]	NT	NT	NT
9	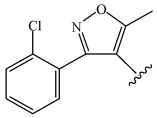	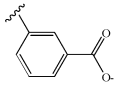	0.79	63	2.5	2.1	1.7
10	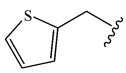	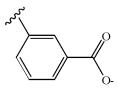	0.064	7.8	0.22	0.057	0.22
10a[a]	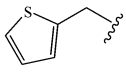	H	7	NT	NT	NT	NT

[a] K_i values accurate to within 20%. [b] From ref *16*. [c] Not tested.

(*26*). All crystals belong to the space group $P2_12_12_1$. Crystals were isomorphous to those of WT*, except for the WT*/Compound **10** complex, which had a different unit cell (Table 2).

Crystallographic Refinement. The phases were determined by molecular replacement using AmoRe (*27*) with the structure of WT* (*25*) as a search model. In each case, a single solution of the translation function was refined in

Table 2: Crystallographic Statistics and Refinement Results

complex	WT*/**2**	WT*/**5**	WT*/**6**	WT*/**10**
space group		$P2_12_12_1$		
unit cell (Å)	41.37; 61.67; 89.40	41.34; 61.66; 89.13	41.29; 58.97; 88.63	72.63; 34.56; 105.36
resolution (Å)[a]	1.90 (1.97−1.90)	1.20 (1.24−1.20)	1.75 (1.81−1.75)	1.60 (1.66−1.60)
wavelength (Å)	1.00000	1.00000	1.00000	0.98012
beamline/detector		APS DND-CAT 5ID-B/MARCCD		
total reflections	97 325	421 106	125 153	220 946
unique reflections	18 289 (1834)	71 168 (6965)	22 129 (2162)	36 330 (3568)
completeness (%)	97.1 (99.1)	99.0 (98.0)	98.3 (97.7)	99.8 (99.5)
R_{merge} (%)	8.7 (32.9)	5.0 (28.9)	5.3 (41.3)	5.3 (24.1)
protein atoms	2026			
ligand atoms	20	16	20	22
solvent[b]	235	494	369	409
R_{cryst}/R_{free} (%)[b]	19.6/23.2	10.6/14.8	17.1/19.8	17.7/19.8
rms bonds (Å)	0.009	0.007	0.009	0.009
rms angles (deg)	1.54	1.46	1.44	1.52

[a] Values in parentheses are for the highest-resolution shell. [b] Including phosphate and potassium ions. [c] R_{free} was calculated with 5% (WT*/**5**) and 10% (WT*/**2**, WT*/**6**, WT*/**10**) of reflections set aside randomly.

CNS (*28*) using rigid-body refinement followed by torsion angle simulated annealing. Several rounds of Cartesian and *B*-factor refinement was followed by manual corrections using $2F_o-F_c$ and F_o-F_c σ_A-weighted maps displayed with TURBO (*29*) until the refinement statistics converged to their final values (Table 2).

The structure of the complex between WT* and compound **5**, which was determined to 1.2 Å resolution, was refined further in SHELX97 (*30*). The refinement was carried out using ADPs (anisotropic displacement parameters) with standard DELU (rigid-bond), SIMU (spatially adjacent atoms), and ISOR (isolated atoms to be approximately isotropic) restraints and converged at R_{cryst}/R_{free} of 12.6/15.6%. The introduction of hydrogen atoms in the model lowered the *R*-factors slightly. At this stage DELU, SIMU, and ISOR restraints were adjusted using the program PARVATI (*31*). The final *R*-factors were 10.6% for R_{cryst} and 14.8% for R_{free} (Table 2).

Synthesis. Compounds **1**−**7** (*16*) and compounds **8**, **9**, and **10** were synthesized as previously described (*18*). All other compounds were used as supplied by the manufacturers without further purification.

Microbiology. Compound **10** was tested for synergy with the β-lactam ampicillin against pathogenic *Staphylococci* from clinical isolates at the Hospital Ramón y Cajal; these bacteria were resistant to β-lactams due to expression of class A β-lactamases. Strains of bacteria tested were: ATTC *Staphylococcal aureus* (Sa) (non-β-lactamase producer), *S. aureus* isolate 22491 (Sa22491) (class A β-lactamase producer), *S. aureus* isolate 23614 (Sa23614) (class A β-lactamase producer), and *S. aureus* isolate 24273 (Sa24273) (class A β-lactamase producer). Also tested were three laboratory strains of K12 *Escherichia coli* transformed with TEM-1 (*E. coli* TEM-1), TEM-15 (*E. coli* TEM-15), and TEM-52 (*E. coli* TEM-52), all expressed off the pALTER plasmid (*25*). Minimum inhibitor concentration (MIC) values were determined with Mueller-Hinton Broth II using the micro-dilution method according to NCCLS guidelines (*32*). Each value reported reflects the average of three independent experiments.

RESULTS

Enzyme Inhibition. All of the boronic acid inhibitors (Table 1) bind reversibly to TEM-1 and its mutants. For the *m*-carboxyphenylglycylboronic acids (**8**, **9**, and **10**) inhibition was time-dependent. For these three, activity displayed classic time-dependent recovery from inhibition in a reaction initiated with substrate (i.e., reaction rates increased after an initial lag-phase before reaching a steady-state plateau). The time-dependence in the inhibition thus reflects a slow off-rate. Consistent with reversibility, the inhibitors could be competed off by increasing substrate concentration. We have accounted for this incubation effect in the K_i values reported for these inhibitors (Methods).

As with the class C β-lactamase AmpC (*18*), adding an *m*-carboxyphenyl group to the glycylboronic acids improved TEM-1 inhibition considerably, by between 25- and 100-fold (compare compound **8** to **8a** or compound **10** to **10a**, Table 1). For the WT enzyme, the addition of the *m*-carboxyphenyl side chain improves binding energy by between 1.9 and 2.8 kcal/mol, with compound **10** reaching a K_i value of 64 nM.

For the ESBL mutants TEM-52 and TEM-64, and for the IRT mutant TEM-32, the trends in affinities were similar to that of TEM-1, though they were typically two to 3-fold worse than for the WT enzyme. There were some exceptions to this rule. For instance, compound **5** was actually 4-fold better versus TEM-52 than it was versus WT, and was 13-fold better versus TEM-52 than it was versus TEM-64. On the other had, compound **7** was 2-fold better versus TEM-64 than it was versus TEM-52 (Table 1). It is interesting to note that compound **5** bears the R1 side chain of cefotaxime and that TEM-52, though classified as having an extended spectrum against 3rd generation cephalosporins in general, is primarily a cefotaximase, with activities 25-fold better for cefotaxime than ceftazidime (*25*, *33*). Correspondingly, compound **7** bears the R1 side chain of ceftazidime, and TEM-64 is an ESBL that has 2-fold greater activity against ceftazidime than it does against cefotaxime (*25*, *34*). The trends in affinities for the transition-state analogues thus appear to mimic the trends in substrate recognition among the mutant enzymes.

The important outlier was the IRT TEM-30, against which the *m*-carboxyphenylglycylboronic acids (**8**, **9**, and **10**) lost 2 orders of magnitude (2.8 kcal/mol) in affinity (Table 1). Thus, compound **10**, which had been the most potent inhibitor of the TEM-1, saw its K_i increase from 0.064 μM to 7.8 μM against TEM-30. In this mutant enzyme Arg244

has been substituted with a serine. This removes a hydrogen bond with the C3(4)′ carboxylate of substrate β-lactams, which the *m*-carboxy group in **8**−**10** was designed to mimic (the hydrogen-bond between Arg244 and the *m*-carboxy group can be observed the WT*/**10** complex, below). On the other hand, the glycylboronic acids (**1**−**7**, **8a**, and **10a**), which lack the m-carboxyphenyl side chain and are less substrate-like than **10**, have undiminished affinity for TEM-30 relative to WT TEM-1.

X-Ray Crystal Structures. To investigate the structural bases for recognition, we determined the crystal structure of TEM-1 in complex with four of the inhibitors, including the high affinity **10** (Table 2). Excluding proline and glycine residues, all amino acids were in the most favored and additionally allowed regions of the Ramachandran plot, except for residue Leu220, which consistently in TEM structures, including one determined at 0.85 Å (*24*), is in a generously allowed region (*35*).

In all structures, the position of the inhibitor in the active site was unambiguously identified in the initial F_o-F_c difference map contoured at 3σ (Figure 3). Electron density connected the Oγ of the catalytic Ser70 to the boron atom of the inhibitors. The boron geometry was tetrahedral, as expected. Compounds **2**, **5**, and **6**, which display only the R1 side chain of β-lactams (Figure 1), adopted a conformation in the active site consistent with acylation transition-state analogues, resembling the structure of a phosphonate transition-state analogue in complex with the class A β-lactamase PC1 from *S. aureus* (*21*) and the ultra-high-resolution structure of compound **7** in complex with WT* (*24*). All three boronic acid complexes overlap well with each other (Figure 4a) (*24*). In these glycylboronic acid structures, the O1 boronic acid hydroxyl hydrogen bonds with the "oxyanion" (*36*) or "electrophilic" (*37*) hole formed by the backbone amide groups of Ser70 and Ala237 (Figure 4b; Table 3). The O2 of the boronic acid hydrogen-bonds with Ser130 and typically an ordered water. The R1 amide group of the inhibitor is placed in the amide recognition region defined by Asn132 and Ala237 (*38*). The R1 amide nitrogen interacts with the backbone oxygen of Ala237 and the R1 amide oxygen interacts with Nδ2 of Asn132. The distal ring that terminates these R1 side chains typically lies in the region of Glu240, though only the exo-cyclic amino group of compound **5** appears to directly hydrogen bond with this residue. The exception is the side chain of compound **2**, whose steric bulk forces it to lie in a different region of the site, forming nonpolar interactions with the side chain of Tyr105 (Figure 4a).

In contrast to compounds **2**, **5**, and **6**, compound **10**, which adds the m-carboxyphenyl group to the glycylboronic acids, adopts a different orientation in the TEM-1 active site (Figure 4c). The WT*/**10** complex resembles that of a related transition-state analogue in complex with TEM-1 (*17*). This latter structure is thought to mimic the deacylation transition state (*14*) rather than the acylation transition state mimicked by **2**, **5**, and **6**. Whereas O1 is still in the "oxyanion" (*36*) or "electrophilic" (*37*) hole, the configuration around the boron has inverted, with the boronic O2 oxygen adopting the opposite pyramidal position as that adopted in by the simpler glycylboronic acids. In its new position, the O2 hydroxyl hydrogen-bonds with the catalytic base Glu166, displacing the ordered, catalytic water (Wat4) (*14*). The phenyl ring of compound **10** stacks with the aromatic ring of Tyr105 in a herringbone geometry, appearing to make quadrupole interactions. The carboxylate of the inhibitor hydrogen-bonds with Arg244 and Ser235 and an ordered water, Wat56, that appears to be highly conserved among TEM structures (*14*, *22*, *39*) (Table 3). These interactions between Arg244, Ser235, and water are also seen to the C3′ carboxylate of β-lactams (*40*), consistent with this inhibitor carboxylate mimicking this ubiquitous substrate group.

Table 3: Polar Interactions among Active Site Residues and between These Residues and the Inhibitors in the Crystal Structures[a]

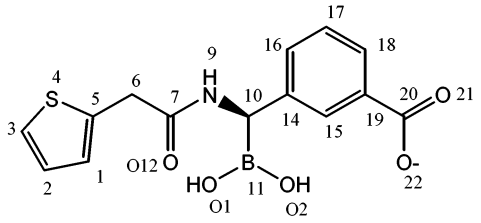

interactions	distance (Å)			
	2	**5**	**6**	**10**
S70N−O1	3.0	2.9	2.9	2.6
A237N−O1	2.8	2.9	2.8	3.1
A237O−N9	4.1	3.5	3.5	3.2
A237O−O1	2.8	2.8	2.8	2.9
S130Oγ−O2	2.6	2.7	2.8	NP
N132Nδ1−O12	2.6	2.9	2.9	2.8
S130Oγ−K234Nζ	3.1	2.8	2.9	2.9
S130Oγ−S70Oγ	3.2	3.1	3.0	3.2
S130Oγ−K73Nζ	3.1	3.3	3.0	3.4
K73Nζ−E166Oϵ2	3.8	3.5	3.8	3.4
K73Nζ−S70Oγ	2.8	2.8	3.0	2.8
Wat1004−E166Oϵ2	2.5	2.6	2.5	NP
Wat1004−N170Oδ1	2.7	2.7	2.8	NP
Wat1004−S70Oγ	2.7	2.7	2.8	NP
N132Oδ1−E166Oϵ2	3.0	2.9	3.2	3.1
N132Oδ1−K73Nζ	2.9	2.7	2.7	2.9
N170Nδ2−E166Oϵ1	2.8	2.8	2.7	2.9
Arg244NH1−O22	NP	NP	NP	3.2
Ser235−O23	NP	NP	NP	2.6

[a] Compound **10** is shown as a reference for numbering.

We wondered if the structure of **10** in complex with WT* would suggest a reason for the slow off-rates these compounds experience in the inhibition assays (above). A common explanation for kinetic barriers to disassociation is reorganization of the enzyme. No significant conformational change in the enzyme was observed either relative to the apo-structure (*41*) or relative to the complexes with the glycylboronic acids **2**, **5**, **6** (this paper), or **7** (*22*), which do not experience an obvious kinetic barrier. Whereas a role for enzyme reorganization cannot be ruled out dynamically, the ground-state structures show little sign of such an effect. On the other hand, reorganization of bound waters and the ligand are apparent. In the crystallographic complex of **10**/WT*, the ordered catalytic water (Wat4) is displaced by the ligand, whereas this water is present in the structures of the glycylboronic acids complexes. Also, the structure of **10** has undergone an inversion of configuration at the boronic acid center relative to the glycylboronic acids; if this inversion occurs on the enzyme, it may also contribute to a kinetic barrier in the binding equilibria.

Microbiology. To investigate the potential of these compounds to reverse antibiotic resistance, we undertook antimicrobial studies in bacterial cell culture. The minimum

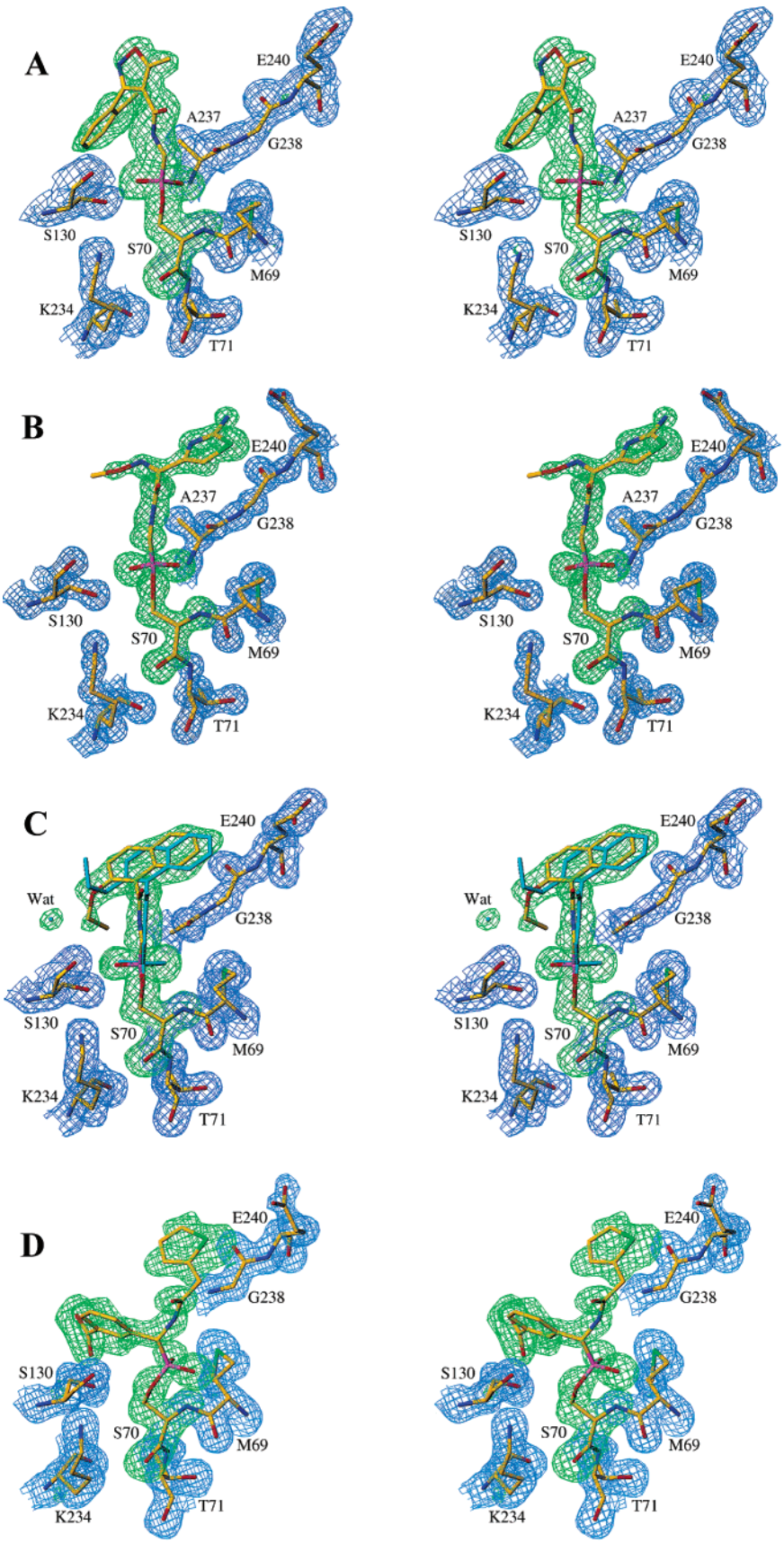

FIGURE 3: Stereoview of electron density for the inhibitors and several active site residues. Fo-Fc simulated annealing omit electron density (green) is shown contoured at 3σ (A, C, and D) and at 5σ (B) for the inhibitors. $2F_o-F_c$ σ_A-weighted electron density (blue) is shown contoured at 1σ (A,C, and D) and at 2σ (B) for surrounding residues. A. Compound **2**. B. Compound **5**. C. Compound **6**. D. Compound **10**. Carbon, nitrogen, oxygen, sulfur, and boron atoms are colored in yellow, blue, red, green, and magenta, respectively.

inhibitory concentration (MIC) values of ampicillin alone against three clinically isolated strains of *S. aureus* producing a class A β-lactamase ranged from 128 to 256 μg/mL. When ampicillin was tested in combination with compound **10**,

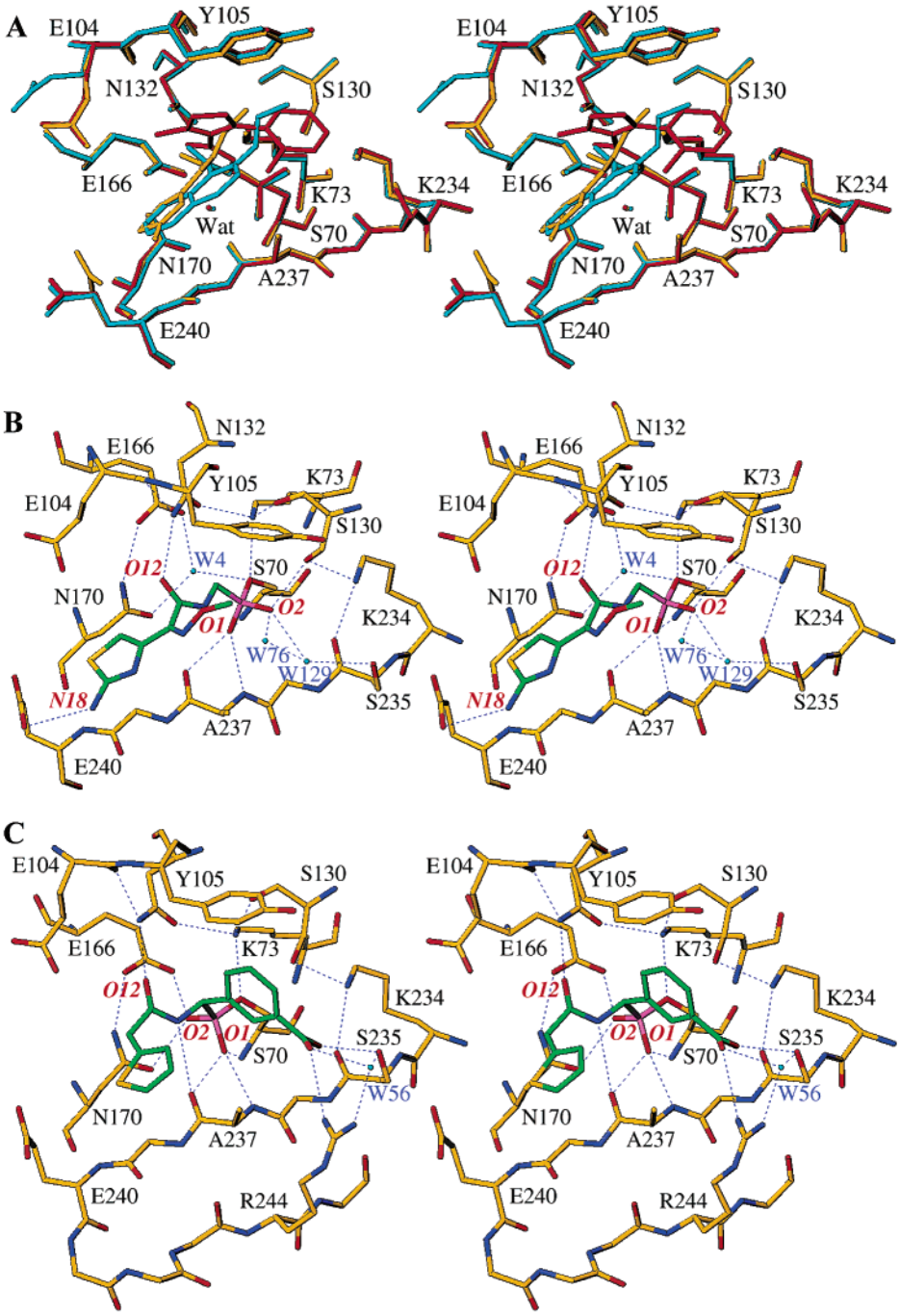

FIGURE 4: Stereoview of the inhibitor complexes in the active site region. A. Superposition of the complexes compounds **2** (red), **5** (yellow), and **6** (cyan). B. Stereoview of hydrogen bond interactions between active site residues and compound **5**, an acylation transition-state analogue. D. Stereoview of hydrogen bond interactions between active site residues and compound **10**, a deacylation transition-state analogue. Atoms of the protein are colored as in Figure 3. Carbon and sulfur atoms of boronic acid compounds are colored green and yellow, respectively. Water molecules are shown as cyan spheres, and hydrogen-bond interactions are depicted as dashed lines. Protein residues, water molecules, and selected atoms of compounds are labeled in black, blue, and red, respectively.

its MIC values improved by between four and 8-fold (Table 4). When tested against a laboratory strain of *E. coli* producing either TEM-1, TEM-15, or TEM-52, ampicillin MIC values improved 64-fold when used in combination with compound **10**. Whereas these inhibitors have not been tested for enzymatic inhibition of the *S. aureaus* enzyme, we note that these enzymes are related and that other boronic acid inhibitors of TEM also inhibit the *S. aureus* enzyme, indeed often with greater affinity (*42*).

DISCUSSION

As this series of transition-state analogues becomes more substrate like, affinity rises for WT TEM-1 β-lactamase. Adding an *m*-carboxyphenyl group, meant to mimic the C3-(4)′ carboxylate of β-lactams, to the glycylboronic acids improves affinity for the TEM enzymes by up to 100-fold, to 64 nM. This improvement appears to owe to hydrogen bonds between the *m*-carboxylate group in compound **10** and residues in the β-lactamase site that typically bind to the

Table 4: Synergy of Compound **10** with Ampicillin against Bacteria Producing Class A β-Lactamases

strain	MIC[a] (μg/mL)	
	AMP[b]	AMP + **10**[c]
Sa[d,e]	2	2
Sa22491[f]	128	32
Sa23614[f]	256	32
Sa24273[f]	256	32
E. coli TEM-1[g]	8192	128
E. coli TEM-15[h]	2048	32
E. coli TEM-52[i]	4096	32

[a] Minimum inhibitory concentration. [b] Ampicillin. [c] The ratio of ampicillin to inhibitor was 2:1; the concentration of AMP is reported. [d] Strains defined in Materials and Methods. [e] *S. aureus*, non-β-lactamase producer. [f] *S. aureus*, class A β-lactamase producer. [g] *E. coli*, TEM-1 producer. [h] *E. coli*, TEM-15 producer. [i] *E. coli*, TEM-52 producer.

ubiquitous C3(4)′ carboxylate of β-lactam substrates, including Arg244 and Ser235 (Figure 4c). Compound **10** is thus one of the few inhibitors to bind well to both class A and class C β-lactamases (*18*), and can greatly increase the sensitivity of resistant bacteria to β-lactams in cell culture (Table 4). The activity of this compound against three of four mutant TEMs, at similar concentrations, is encouraging.

The other side of this coin is that as this series becomes more substrate-like, it appears to fall victim to at least one β-lactamase resistance mutant. TEM-30 (R244S) was selected by the use of clavulanate in the clinic and appears to work by disrupting the hydrogen bond between Arg244 and the C3′ carboxylate of this β-lactam (*39*, *43*, *44*). Disrupting this interaction may misorient clavulanate in the binding site, reducing off-pathway reactions necessary for formation of an irreversible adduct (*22*). Since the *m*-carboxyphenyl group, which is responsible for the improved affinity of compound **10**, mimics this C3′ carboxylate, it is in retrospect unsurprising that TEM-30 is less inhibited by this compound than is TEM-1.

Of mechanistic interest is the differential binding of the transition-state analogues. The TEM-catalyzed hydrolysis of β-lactams begins with the formation of a pre-covalent encounter complex (Figure 2A), which is rapidly attacked by the nucleophilic Ser70. The reaction proceeds through an acylation transition state (Figure 2B) that collapses to a relatively stable acyl adduct (Figure 2C). The catalytic water (Water 4 in this study), activated by Glu166, attacks this acyl intermediate to form a deacylation transition state (Figure 2D) that collapses to form an enzyme−product complex (Figure 2E), followed byproduct disassociation to regenerate the free enzyme. Transition-state analogues that lack the *m*-carboxyphenyl side chain (compounds **1**−**7**, **8a**, and **10a**) bind very differently than transition-state analogues that possess this side chain (compounds **8**, **9**, and **10**), presumably reflecting either the acylation or deacylation transition-state structures. The structures of four glycylboronic acids that lack this *m*-carboxyphenyl group have been determined with TEM β-lactamases (see also (*22*, *24*)). All bind similarly. A key mechanistic feature of these complexes is that the O2 boronic oxygen is oriented away from the deacylating water (Wat4) and toward Ser130, which is thought to activate the lactam nitrogen for leaving in the acylation step of the reaction. These features resemble the structure of a previously determined phosphonate analogue bound to a related class A β-lactamase determined by Herzberg, Pratt, and colleagues (*21*). Following these authors, we consider these structures to be analogues of the acylation transition state (Figure 2B). Adding the *m*-carboxyphenyl to these glycylboronic acids causes the boronic acid group of compound **10** to invert, changing the stereochemistry of the boronic acid in the site. The O2 boronic oxygen of **10** is now found on the opposite side of the boron, where it displaces the catalytic Wat4 and hydrogen-bonds directly to the catalytic base, Glu166. These interactions closely resemble those of analogous boronic acids bound to TEM-1 determined by Strynadka and colleagues (*14*, *17*). Following these authors, we therefore consider these to be analogues of the deacylation transition state (Figure 2D).

These analogues resemble each other closely enough to allow one to identify what distinguishes acylation from deacylation transition-state mimics. It seems that interactions with the carboxylic acid of compound **10**, and by extension the C3(4)′ carboxylate of substrates, is a key recognition determinant for deacylation transition states in class A β-lactamases. Superimposing these transition-state analogue complexes with that of a substrate (*40*) gives a structural view of the reaction coordinate, from acylation transition-state to the previously determined acyl-intermediate (*40*) to the deacylation transition-state (Figure 2B−D). The expected umbrella inversions of configuration between the tetrahedral acylation transition state and the planar acyl-intermediate, and between the planar intermediate and the deacylation transition state, are evident (Figure 5). This inversion results in the movement of the boronic O2 oxygen from the acylation transition-state analogues (Figure 4B), where this atom represents the position of the lactam nitrogen leaving group, to its position in the deacylation transitions state analogues, where the O2 represents the position of the deacylating water as it attacks the acyl center (Figure 4C).

We return, finally, to our original question: confronted by an enzyme prone to resistance mutations, is it better to design inhibitors that resemble the substrate or to design inhibitors dissimilar to the substrate? The most substrate-like of the inhibitors considered here is compound **10**, which approaches an atom-by-atom transition-state analogue for cephalothin (Figure 1D,F). An attractive feature of this compound is its high affinity for WT TEM-1, as is its efficacy in cell culture (Table 4). It has an unusually broad spectrum of activity, inhibiting both class A and class C β-lactamases (*18*) and several mutant TEM enzymes. In these aspects the compound is a good lead compound for drug design to reverse antibiotic resistance to the β-lactams.

If compound **10** has a tragic flaw, it is that it has gained its affinity by resembling the substrate, and this has made it vulnerable to mutant enzymes such as TEM-30 (Table 1). TEM-30 has been selected by the use of clavulanate and related inhibitors, and is widespread in clinical infections. Therapeutic use of **10** should thus rapidly select for TEM-30. This result contrasts with those of Varghese, Colman and colleagues with inhibitors of influenza neuraminadase, where the most substrate-like inhibitors were the least susceptible to two different mutant enzymes selected by related transition-state analogues (*3*). How might these results be reconciled?

One possible explanation is that β-lactams and β-lactamase inhibitors have a much longer history in the clinic than do neuraminidase inhibitors, and so simply more mutants have

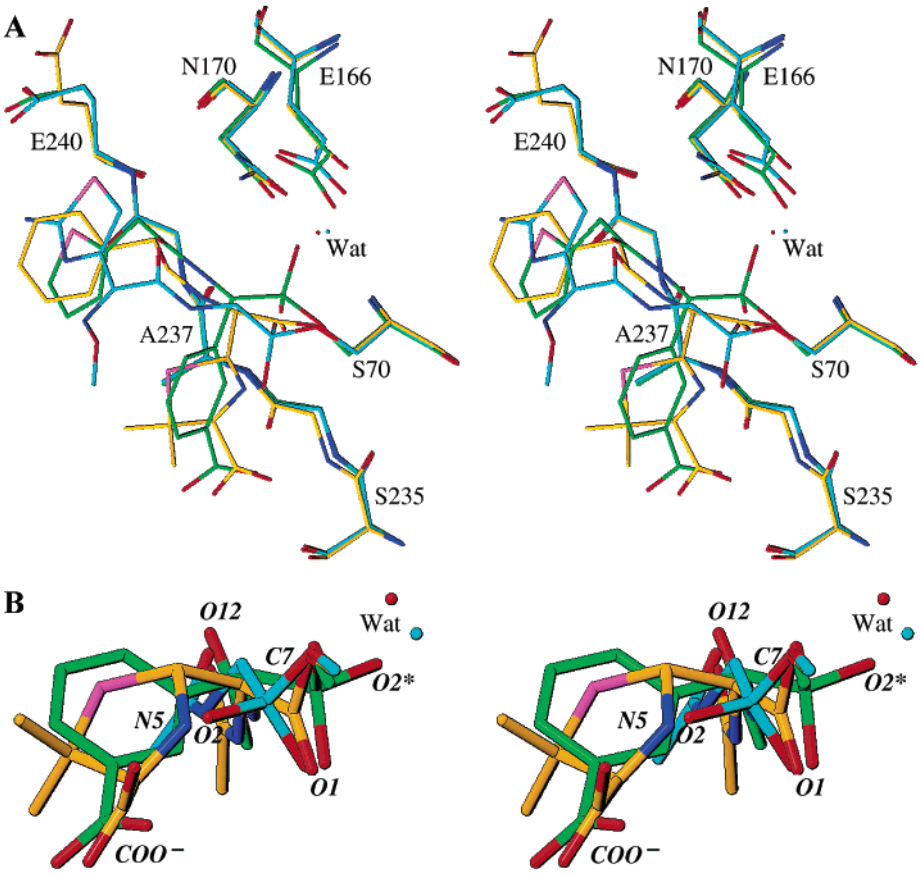

FIGURE 5: The change in geometry around the reactive center as the reaction progresses from acylation high-energy intermediate to acyl−enzyme complex to deacylation high-energy intermediate. A. Stereoview of the superposition of the WT*/**5** (carbon atoms in cyan), TEM-1/penicillin G acyl intermediate (*40*) (carbon atoms in yellow), and WT*/**10** complexes (carbon atoms in green). B. Close-up view of the reaction center. Nitrogen, oxygen, and sulfur atoms are colored in blue, red, and magenta, respectively.

been explored. Indeed, clavulanate is a natural product of evolutionary warfare from *Streptomyces clavulageris* and β-lactamase-producing bacteria have been exposed to this inhibitor over geologic time. On the other hand, TEM-1 is converted into TEM-30 by only a single substitution (Arg244→Ser), and many related mutants have been isolated in the clinic (e.g, the IRTs TEM-31 (R244C), TEM-41 (R244T), TEM-44 (R244S), TEM-51 (R244H), TEM-54 (R244L), and TEM-79 (R244G)), suggesting that substitutions at this position are easy to select. Another explanation is that it might be *even* easier to find mutants for novel inhibitors than it is for substrate analogues. As Vargese, Colman, and colleagues point out (*3*), the mutants to the neuraminidase transition-state analogues sacrifice some of their intrinsic enzyme activity to gain resistance, and the same is certainly true of TEM-30 and other TEM mutants (*25*). Genuinely novel inhibitors, dissimilar to the substrate, might not force this tradeoff (*3*). To investigate this hypothesis, it will be necessary to test more diverse inhibitors against a broader spectrum of the extant mutants.

What can be said at this point is that whereas affinity and enzyme spectrum improve with substrate-similarity in this series of inhibitors, substrate similarity is no sure protection from resistance mutants. The "substrate-analog" hypothesis for inhibitor design may yet prove to be the best strategy when confronting shifting targets. Our results suggest that more research is warranted to address this key problem in an age of widespread antimicrobial resistance.

Data Deposition. The coordinates for the TEM complexes with compounds **2**, **5**, **6**, and **10** here have been deposited with the Protein Data Bank as 1NYY, 1NYM, 1NY0, and 1NXY, respectively.

ACKNOWLEDGMENT

We thank P. Focia, J. Horn, T. Roth, and S. McGovern for reading this manuscript. X-ray crystallographic data were collected at the DuPont-Northwestern-Dow Collaborative Access Team (DND-CAT) synchrotron Research Center at the Advanced Photon Source (APS). DND-CAT is supported by the DuPont Co., the Dow Chemical Co., National Science Foundation, and the State of Illinois. We also thank the R.H. Lurie Cancer Center for support of the NU Structural Biology Center.

REFERENCES

1. Condra, J. H., Schleif, W. A., Blahy, O. M., Gabryelski, L. J., Graham, D. J., Quintero, J. C., Rhodes, A., Robbins, H. L., Roth, E., Shivaprakash, M., Titus, D., Yang, T., Hedy, T., Squires, K. E., Deutsch, P. J., and Emini, E. A. (1995) *Nature 374*, 569−571.
2. Livermore, D. M. (1995) *Clin. Microbiol. Rev. 8*, 557−84.
3. Varghese, J. N., Smith, P. W., Sollis, S. L., Blick, T. J., Sahasrabudhe, A., McKimm-Breschkin, J. L., and Colman, P. M. (1998) *Structure 6*, 735−46.
4. Abraham, E. P., and Chain, E. (1944) *Nature 146*, 837.
5. Matagne, A., Dubus, A., Galleni, M., and Frere, J. M. (1999) *Nat. Prod. Rep. 16*, 1−19.

6. Smith, G. M., Abbott, K. H., Wilkinson, M. J., Beale, A. S., and Sutherland, R. (1991) *J. Antimicrob. Chemother. 27*, 127−36.
7. O'Callaghan, J. P., Chess, Q., McKimmey, C., and Clouet, D. H. (1979) *J Pharmacol. Exp. Ther. 210*, 361−7.
8. Knowles, J. R. (1985) *Acc. Chem. Res. 18*, 97−104.
9. Yang, Y., Rasmussen, B. A., and Shlaes, D. M. (1999) *Pharmacol. Ther. 83*, 141−151.
10. Matagne, A., and Frere, J. M. (1995) *Biochim. Biophys. Acta 1246*, 109−27.
11. Knox, J. R. (1995) *Antimicrob. Agents Chemother. 39*, 2593−2601.
12. Rice, L. B., Carias, L. L., Hujer, A. M., Bonafede, M., Hutton, R., Hoyen, C., and Bonomo, R. A. (2000) *Antimicrob. Agents Chemother. 44*, 362−7.
13. Crompton, I. E., Cuthbert, B. K., Lowe, G., and Waley, S. G. (1988) *Biochem. J. 251*, 453−9.
14. Strynadka, N. C., Jensen, S. E., Alzari, P. M., and James, M. N. (1996) *Nat. Struct. Biol. 3*, 290−7.
15. Weston, G. S., Blazquez, J., Baquero, F., and Shoichet, B. K. (1998) *J. Med. Chem. 41*, 4577−86.
16. Caselli, E., Powers, R. A., Blasczcak, L. C., Wu, C. Y., Prati, F., and Shoichet, B. K. (2001) *Chem. Biol. 8*, 17−31.
17. Ness, S., Martin, R., Kindler, A. M., Paetzel, M., Gold, M., Jensen, S. E., Jones, J. B., and Strynadka, N. C. (2000) *Biochemistry 39*, 5312−21.
18. Morandi, F., Caselli, E., Morandi, S., Focia, P. J., Blazquez, J., B. K. Shoichet, and Prati, F. (2003) *J. Am. Chem. Soc. 125*, 685−695.
19. Rahil, J., and Pratt, R. F. (1994) *Biochemistry 33*, 116−25.
20. Li, N., Rahil, J., Wright, M. E., and Pratt, R. F. (1997) *Bioorg. Med. Chem. 5*, 1783−8.
21. Chen, C. C., Rahil, J., Pratt, R. F., and Herzberg, O. (1993) *J. Mol. Biol. 234*, 165−78.
22. Wang, X., Minasov, G., and Shoichet, B. K. (2002) *J. Biol. Chem. 277*, 32149−56.
23. Wang, X., Minasov, G., and Shoichet, B. K. (2002) *Proteins 47*, 86−96.
24. Minasov, G., Wang, X., and Shoichet, B. K. (2002) *J. Am. Chem. Soc. 124*, 5333−40.
25. Wang, X., Minasov, G., and Shoichet, B. K. (2002) *J. Mol. Biol. 320*, 85−95.
26. Otwinowski, Z., and Minor, W. (1997) *Methods Enzymol. 276*, 307−326.
27. Navaza, J. (1994) *Acta Crystallogr., Sect. A 50*, 157−163.
28. Brünger, A. T., Adams, P. D., Clore, G. M., DeLano, W. L., Gros, P., Grosse-Kunstleve, R. W., Jiang, J. S., Kuszewski, J., Nilges, M., Pannu, N. S., Read, R. J., Rice, L. M., Simonson, T., and Warren, G. L. (1998) *Acta Crystallogr., Sect. D 54*, 905−921.
29. Cambillau, C., and Roussel, A. (1997) *Turbo Frodo*, ed. OpenGL, Universite Aix-Marseille II: Marseille, France.
30. Sheldrick, G. M., and Schneider, T. R. (1997) *Methods Enzymol. 277*, 319−343.
31. Merritt, E. A. (1999) *Acta Crystallogr., Sect. D 55*, 1109−17.
32. C. f. C. L. S. National (1997) *Methods for Dilution Antimicrobial Susceptibility Tests for Bacteria that Grow Aerobically. Approved Standard M7-A4*, National Committee for Clinical Laboratory Standards, Villanova, PA, Vol. 17.
33. Poyart, C., Mugnier, P., Quesne, G., Berche, P., and Trieu-Cuot, P. (1998) *Antimicrob. Agents Chemother. 42*, 108−13.
34. Vakulenko, S. B., Taibi-Tronche, P., Toth, M., Massova, I., Lerner, S. A., and Mobashery, S. (1999) *J. Biol. Chem. 274*, 23052−60.
35. Laskowski, R. A., MacArthur, M. W., Moss, D. S., and Thornton, J. M. (1993) *J. Appl. Crystallogr. 26*, 283−291.
36. Murphy, B. P., and Pratt, R. F. (1988) *Biochem. J. 256*, 669−72.
37. Usher, K. C., Blaszczak, L. C., Weston, G. S., Shoichet, B. K., and Remington, S. J. (1998) *Biochemistry 37*, 16082−92.
38. Powers, R. A., and Shoichet, B. K. (2002) *J. Med. Chem. 45*, 3222−34.
39. Swaren, P., Golemi, D., Cabantous, S., Bulychev, A., Maveyraud, L., Mobashery, S., and Samama, J. P. (1999) *Biochemistry 38*, 9570−9576.
40. Strynadka, N. C., Adachi, H., Jensen, S. E., Johns, K., Sielecki, A., Betzel, C., Sutoh, K., and James, M. N. (1992) *Nature 359*, 700−705.
41. Voladri, R. K., Tummuru, M. K., and Kernodle, D. S. (1996) *J. Bacteriol. 178*, 7248−53.
42. Tondi, D., Powers, R. A., Caselli, E., Negri, M. C., Blazquez, J., Costi, M. P., and Shoichet, B. K. (2001) *Chem. Biol. 8*, 593−611.
43. Zafaralla, G., Manavathu, E. K., Lerner, S. A., and Mobashery, S. (1992) *Biochemistry 31*, 3847−3852.
44. Moews, P. C., Knox, J. R., Dideberg, O., Charlier, P., and Frere, J. M. (1990) *Proteins 7*, 156−171.

BI034242Y